View metadata, citation and similar papers at core.ac.uk

brought to you by CORE

provided by Juelich Shared Electronic Resources

On the Parametrisation of Lattice Boltzmann Method in Pore-Scale Flow Simulations

S. Khirevich, U. Tallarek

published in

NIC Symposium 2016
K. Binder, M. Müller, M. Kremer, A. Schnurpfeil (Editors)

Forschungszentrum Jülich GmbH,
John von Neumann Institute for Computing (NIC),
Schriften des Forschungszentrums Jülich, NIC Series, Vol. 48,
ISBN 978-3-95806-109-5, pp. 389.
http://hdl.handle.net/2128/9842

© 2016 by Forschungszentrum Jülich
Permission to make digital or hard copies of portions of this work for personal or classroom use is granted provided that the copies are not made or distributed for profit or commercial advantage and that copies bear this notice and the full citation on the first page. To copy otherwise requires prior specific permission by the publisher mentioned above.

On the Parametrisation of Lattice Boltzmann Method in Pore-Scale Flow Simulations

Siarhei Khirevich[1,2] **and Ulrich Tallarek**[1]

[1] Department of Chemistry, Philipps-Universität Marburg, 35032 Marburg, Germany
E-mail: {khirevic, tallarek}@staff.uni-marburg.de

[2] Upstream Petroleum Engineering Research Center, KAUST,
Thuwal 23955-6900, Kingdom of Saudi Arabia
E-mail: siarhei.khirevich@kaust.edu.sa

We analyse impact of parametrisation in lattice Boltzmann simulations of flow in complex geometries. For the input geometries we use four sets of regularly and irregularly packed spheres ("packings") with known accurate solution for the permeability or drag. All four geometries have porosity equal to 0.366 but different microstructure resulting in their different permeability values. We vary spatial resolution in the range between 5 and 750 lattice nodes per sphere diameter, observe different behaviour of the numerical error for several resolution sub-ranges and address them in detail providing practical guidelines for increasing accuracy in low-resolution simulations, which are typical for practical problems.

1 Introduction

Transport processes (such as flow or diffusion) in porous media occur in many diverse fields of science and engineering, and their accurate prediction and optimisation requires understanding, both qualitative and quantitative, of the underlying physical phenomena. Slow (Stokes) flow of a viscous fluid is one of such key processes, and computer simulations nowadays are promising tools for its study. Among others, the lattice Boltzmann method (LBM) became a powerful computer simulation approach for, in particular, simulations of flows in complex geometries[3].

LBM is based on evolution of a "lattice gas", where classical gas model representation is replaced by the one with discrete space and time: individual molecules are combined into fluxes which do exist at discrete lattice nodes and move along prescribed discrete links connecting each node with its neighbours. During discrete time steps fluxes do propagate between lattice nodes and collide at them. Output of the collision step as well as the simulation result depend on a particular selection of LBM adjustable parameters (relaxation rates).

Despite more than two decades of the method history, there is still a controversy about selection of its parameters even for such a "simple" underlying physical phenomenon as Stokes flow of incompressible isothermal fluids, when we consider complex geometries like porous media. In this study we approach this problem using for the input geometry packing of impermeable spheres densely packed in regular and irregular fashions. We simulate Stokes flow in the voids between spheres, and assess method accuracy against its parametrisation.

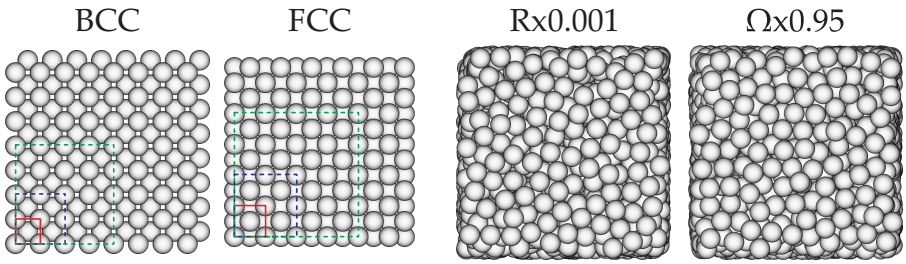

Figure 1. Simulation geometries: sets of spheres (packings) of equal size where spheres are arranged in regular (BCC, FCC) and irregular (Rx0.001, Ωx0.95) fashions; all four packings have equal void space fraction of $\varepsilon = 0.366$. Irregular packings contain about 7000 spheres each.

2 Numerical Simulation Approach

2.1 Input Geometry

We create assemblies of fixed in space, impermeable spheres arranged in regular and irregular (random) fashions, considering two packings for each one. All four packings are spatially periodic and have equal porosity of $\varepsilon = 0.366$, the value close to the ones occurring in many real systems. We intentionally fix porosity to address the impact of heterogeneity on the simulation accuracy while it is assumed that irregular geometries may have lower numerical errors due to "error cancellation" effects. Coordinates of spheres in the regular packings are calculated analytically: first we create standard face-centred and body-centred packings of touching spheres with porosities of ≈ 0.26 and ≈ 0.32, respectively, and then shrink the sphere radii to obtain the target porosity of 0.366. Irregular packings were generated using Jodrey–Tory[2] and Monte-Carlo algorithms which are geometrical approaches to distribute spheres in space in irregular fashion while achieving lower porosities ($\varepsilon < 0.40$). These four packings allowed us to create geometries – comprised of identical objects – with equal average porosity but different microstructure and different values of permeability/drag.

2.2 Discretisation Procedure

One of the key differences of this study from previous works is the discretisation procedure. Standard LBM approaches operate with uniform cubic meshes, and to simulate flow in a given packing its geometry is mapped onto the corresponding domain with cubic mesh marking each mesh node as "solid" or "fluid". In the case of a packing with small amount of spheres (say, less than 10) and low discretisation resolution d_{sp} (≈ 10 or fewer lattice nodes per sphere diameter) the change in the simulated permeability/drag value during step-by-step increase of the domain dimensions can be quite large[1]. In this study we replicate considered geometries using their periodicity property and then discretise it. After proper selection of the domain dimensions such approach allows us to create meshes with non-integral dimensions of the initial unit cell and results in dramatic reduction of a scatter in simulated transport coefficients (i.e. drag or permeability)[1].

2.3 Flow Simulation Approach: The Lattice Boltzmann Method

For the simulations of Stokes flow we use the lattice Boltzmann method (LBM), a suitable approach for simulations of flows in complex geometries. LBM is based on the evolution of a "lattice gas" consisting of distribution functions of gas molecule fluxes along a prescribed discrete set of lattice links (19 in this study) connecting each lattice node with its neighbours. Each LBM iteration consists of two steps: i) propagation of fluxes between lattice nodes along lattice links (streaming step), and ii) collision of fluxes at each lattice node (collision step). In LBM simulations with the course of time its distribution function (of fluxes) iteratively approaches an equilibrium, and simulation is done after variation of the distribution function becomes sufficiently small. The streaming step is a universal one for various LBM models, while implementation of the collision may differ. A simple and commonly used version of the collision operator is so-called "BGK"[4], which contains only one relaxation time τ defining the decay rate of the function towards its equilibrium as well as the viscosity of the simulated fluid. In the case of using so-called "bounce-back" boundary condition (a *de facto* approach for simulations based on micro-CT images of complex medium), a well known drawback of LBM BGK is its dependency of the simulated permeability on τ[6].

Recent developments of LBM models resulted in collision operators with collision occurring in the space of hydrodynamic and kinetic moments (like density, momentum, energy, energy flux), with corresponding conversion of the distribution function to/from the momentum space. Such a formulation of the collision operator[7] allows introduction of multiple (up to the amount of links per lattice node, or 19 in this study, $\tau_{0\ldots18}$) relaxation times – so-called MRT collision operator – for each individual mode, which also poses a question on the particular selection of those parameters, remaining unanswered till now. However, it is suggested that for Stokes simulations individual adjustment of all MRT relaxation rates is not necessary, and in the case of properly grouping the relaxation rates only two prescribed values τ_ν, τ_f are sufficient to provide viscosity independent simulations of permeability. Namely, in this case the multiple-relaxation-time collision operator is reduced to two-relaxation-time (TRT) where, from the point of simulations, τ_ν controls fluid viscosity while τ_f remains apparently free. However, it was demonstrated that when the following combination of these relaxation parameters $\Lambda = (\tau_\nu - 1/2)(\tau_\mathrm{f} - 1/2)$ stays fixed, LBM results in viscosity-independent permeability up to machine accuracy in any geometry[5,6]. Mathematical analysis of LBM behaviour for the simple case of flow between two parallel plates (Poiseuille flow) revealed that Λ controls the location of the zero-velocity boundary between adjacent solid and fluid voxels, and there are some specific values of Λ for this geometry: $\Lambda = 3/16$ results in correct boundary location for horizontally-oriented open channel while $\Lambda = 3/8$ – for diagonal orientation; $\Lambda = 1/8$ gives analytical (up to machine accuracy) flow velocity for horizontal orientation. Analysis of more complex geometries still remains an open topic, and therefore we consider four "basic" values of $\Lambda = 1/8, 3/16, 3/8$, and $1/4$ – the latter providing results of widely used BGK collision with $\tau = 1$ – as well as wider variation of Λ between $1/512$ and 2.

Here our value of interest is the average drag (F_d) exerted on a sphere, which can be seen as the quantity opposite to permeability (k): for a given geometry higher drag means lower permeability, and, in other words, higher resistance of a given geometry to the flow. Drag and permeability are related as $F_\mathrm{d} = \frac{d_\mathrm{sp}^2}{18(1-\varepsilon)k}$. For the reference values of drag $F_\mathrm{d}^\star$ we use the accurately determined ones from our previous study[1].

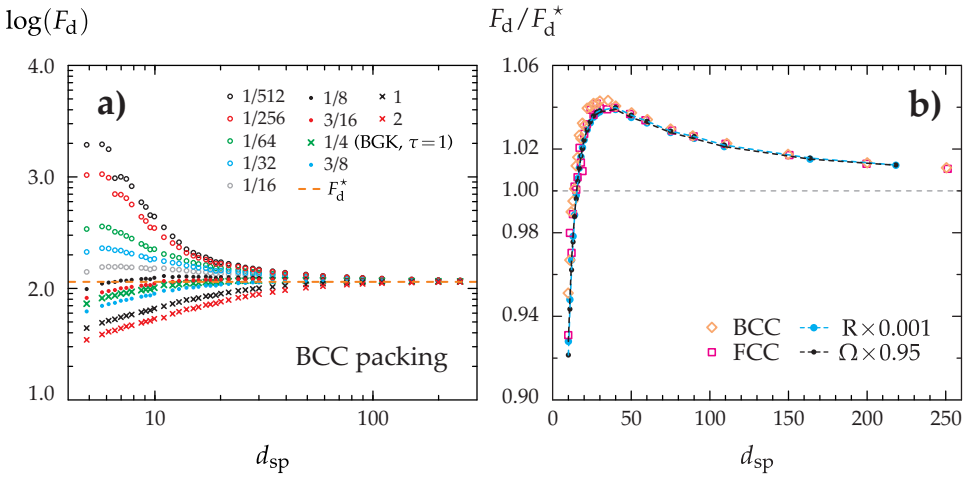

Figure 2. a) Dependence of F_d on discretisation resolution (d_sp) in BCC packing; all other packing types (FCC, Rx0.001, Ωx0.95) demonstrate a very similar picture (not shown). b) Convergence of the relative drag $F_\mathrm{d}/F_\mathrm{d}^\star$ calculated as average from 4 "basic" Λ values ($1/8$, $3/16$, $1/4$, $3/8$); all packing types are shown.

2.4 General Impact of Mag on Drag

We start our analysis by addressing the impact of Λ using one of the regular packings (BCC). The results (Fig. 2a) reveal crucial influence of Λ on drag at lower spatial resolutions: variation of Λ may lead to ten-fold over- or underestimation of the accurate value. A similar picture is observed for other three packings[1] (not shown). Convergence towards $F_\mathrm{d}^\star$ vs. spatial resolution can be non-monotonous, and its behaviour strongly depends on the particular Λ value. On the next step we took four "basic" values ($1/8$, $3/16$, $1/4$, $3/8$) and calculated the average drag for them. The results shown in Fig. 2b confirm non-monotonous convergence: at low resolutions LBM underestimates $F_\mathrm{d}^\star$, then the numerical solution crosses the accurate value and hereafter starts very slow convergence from above. Such a behaviour was observed in various previous works but interpreted differently (suggesting no convergence at all at higher resolutions[8] or attributing a low-resolution branch of the curve to the discrete porosity error[9], which, in turn, is significantly lower in this study[1] compared to the work of Maier *et al.*[9]). Fig. 2b motivates to split the following analysis into higher ($d_\mathrm{sp} > 30$) and lower ($d_\mathrm{sp} < 30$) resolution regions.

2.5 Analysis of High-Resolution Region

A closer examination of the high-resolution region in Fig. 2a is shown in Fig. 3a,b, where very similar behaviour in relative drag $F_\mathrm{d}/F_\mathrm{d}^\star$ is shown for one regular (BCC) and one irregular (Rx0.001) packings. As both panels a) and b) of Fig. 3 reveal, drag values calculated with all considered Λ values collapse to each other above $F_\mathrm{d}^\star$, and similar behaviour is observed for the other two packings (not shown). For the whole range $\Lambda \in [1/512, 2]$ variation of Λ beyond "basic" values of $\Lambda \in [1/8, 3/8]$ does not change the picture qualitatively: for all Λ the solution crosses its accurate value $F_\mathrm{d}^\star$, meaning that with an increase of resolution a numerical solution obtained for arbitrary large value of Λ will cross $F_\mathrm{d}^\star$.

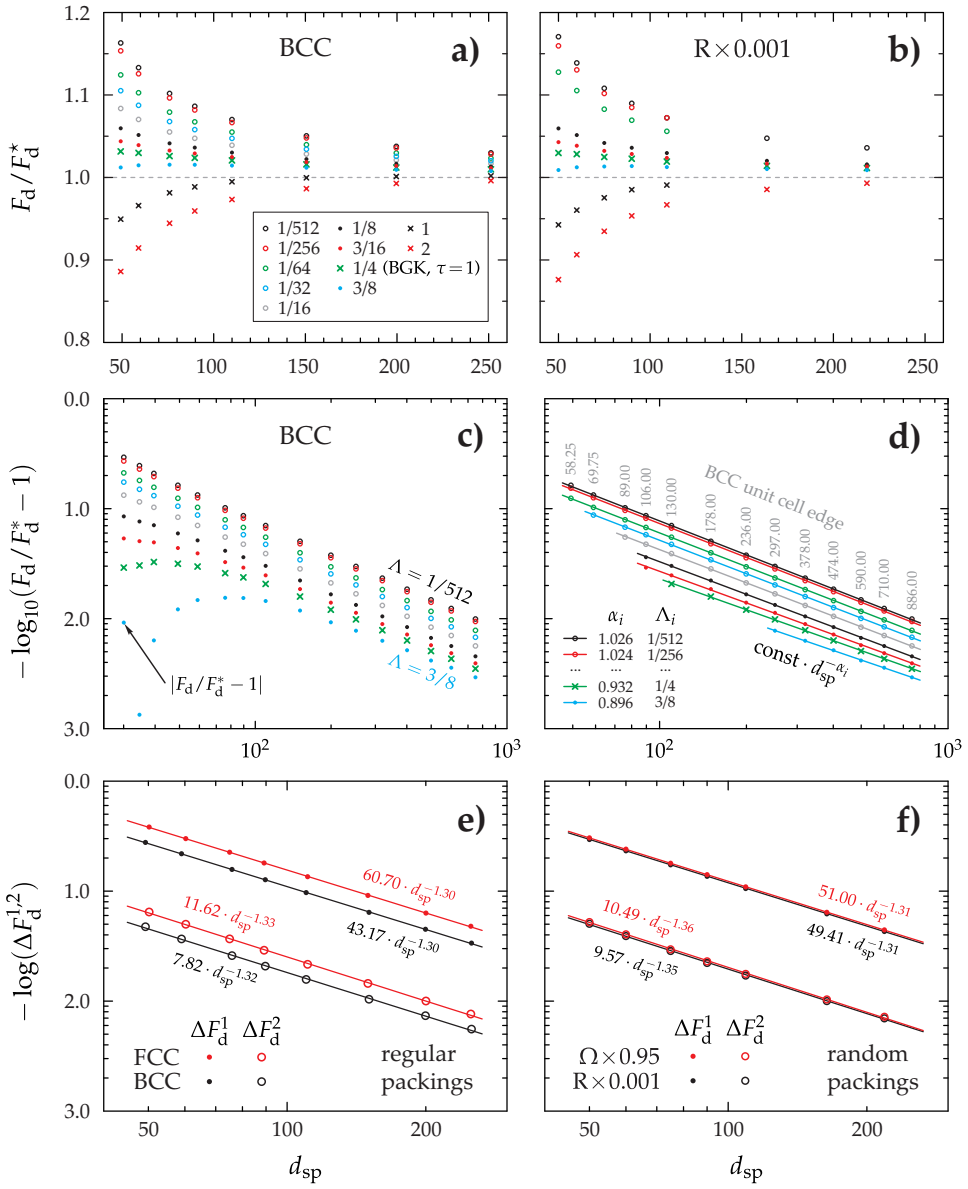

Figure 3. a, b) Dependence of the normalised drag $F_d/F_d^\star$ on discretisation resolution at high resolution values for one regular (BCC) and one irregular (Rx0.001) packing. c) The same as b) but with further resolution increase and log-log axis scale. d) Particular points extracted from c) with the corresponding power law fits; inset shows scaling exponents. e) and f) Differences between drag values ΔF_d^i calculated with Λ pairs of $(1/512, 2)$ and $(1/8, 3/8)$ for all packing types: $\Delta F_d^1 = (F_d^{\Lambda=1/512} - F_d^{\Lambda=2})/F_d^\star$ and $\Delta F_d^2 = (F_d^{\Lambda=1/8} - F_d^{\Lambda=3/8})/F_d^\star$.

Panel c) in Fig. 3 shows the drag error on a double-logarithmic scale. Note that we keep the error sign (except one indicated point) and did not plot its negative values. Log-

log scale clearly demonstrates transient convergence rate of larger Λ values, and for larger Λ a constant convergence rate is observed for higher resolution values. Partially observed constant convergence rates motivate to perform fitting only for the corresponding curve regions, which is shown in Fig. 3d. The obtained convergence rates are -1.0 or slower indicating that selection of larger Λ on the one hand may result in lower absolute errors at high resolutions, but on the other hand approximately constant convergence rates are observed at much higher resolution as well as the rates of convergence becomes slower.

It is straightforward to address convergence of the relative difference in the drag simulated for various Λ values. For this purpose we took two pairs of limiting values: $[1/512, 2]$ for the whole considered Λ range and $[1/8, 3/8]$ for the "basic" Λ values only such that $\Delta F_{\mathrm{d}}^{1} = (F_{\mathrm{d}}^{\Lambda=1/512} - F_{\mathrm{d}}^{\Lambda=2})/F_{\mathrm{d}}^{\star}$ and $\Delta F_{\mathrm{d}}^{2} = (F_{\mathrm{d}}^{\Lambda=1/8} - F_{\mathrm{d}}^{\Lambda=3/8})/F_{\mathrm{d}}^{\star}$. Our results reveals almost identical convergence rate of ~ 1.3 for all four packings types as well as for two considered difference intervals. This allows to conclude that with the increase of resolution the drag values obtained with virtually any pair of Λ will first collapse to some value above $F_{\mathrm{d}}^{\star}$ and then continue its slow convergence to $F_{\mathrm{d}}^{\star}$ from above.

2.6 Analysis of Low-Resolution Region

Low discretisation resolutions are common in practical LBM simulations[10,11]. As Fig. 4 shows, Λ has a strong and dispersive impact on the simulated drag values. On the other hand, even for the lower resolution case its impact on the relative drag $F_{\mathrm{d}}/F_{\mathrm{d}}^{\star}$ is almost identical for all four packings. We note that thanks to our improved discretisation approach one can see systematic trends in drag behaviour for $d_{\mathrm{sp}} < 20$ in regular packings. Drag obtained with the basic Λ values $[1/8, 3/8]$ systematically under- and then overestimates the accurate value $F_{\mathrm{d}}^{\star}$. At the same time F_{d} obtained for Λ values out of the basic region are strictly lower or higher than $F_{\mathrm{d}}^{\star}$, suggesting to use this property and to calculate a new value of F_{d} taking the average of drag values obtained for Λ out of the basic range. Among initially chosen Λ values the lowest total error demonstrated the pair of $\Lambda = 1$ and $\Lambda = 1/16$ with the resulting average drag indicated by solid black line in Fig. 4: except for very low spatial resolutions $d_{\mathrm{sp}} < 10$ such averaging of two simulations with different Λ improves the final simulation accuracy.

3 Conclusion

We performed simulations of Stokes flow using two-relaxation-time (τ_ν and τ_{f}) LBM with bounce-back boundary condition, taking as input geometries two regular and two irregular packings of equal spheres fixing their porosity to $\varepsilon = 0.366$. Such a choice of geometries allowed us to study systems with relatively complex pore space and at the same time accurately determined reference permeability/drag values. We studied the impact of the specific combination of LBM relaxation times $\Lambda = (\tau_\nu - 1/2)(\tau_{\mathrm{f}} - 1/2)$ which controls spatial location of zero-velocity boundary in flow simulations. Λ was varied within the wide range of $[1/512, 2]$, giving additional attention to the "basic" values of $1/4$ (widely used in BGK LBM simulations) as well as $1/8$, $3/16$, $3/8$ which provide exact velocity profiles or average flow rate in slit channel geometry accessible for direct analytical analysis. The "basic" Λ values did not provide any additional gain in accuracy, and fall into the general pattern of solutions with other values from $\Lambda \in [1/512, 2]$. Due to the dispersive impact of Λ

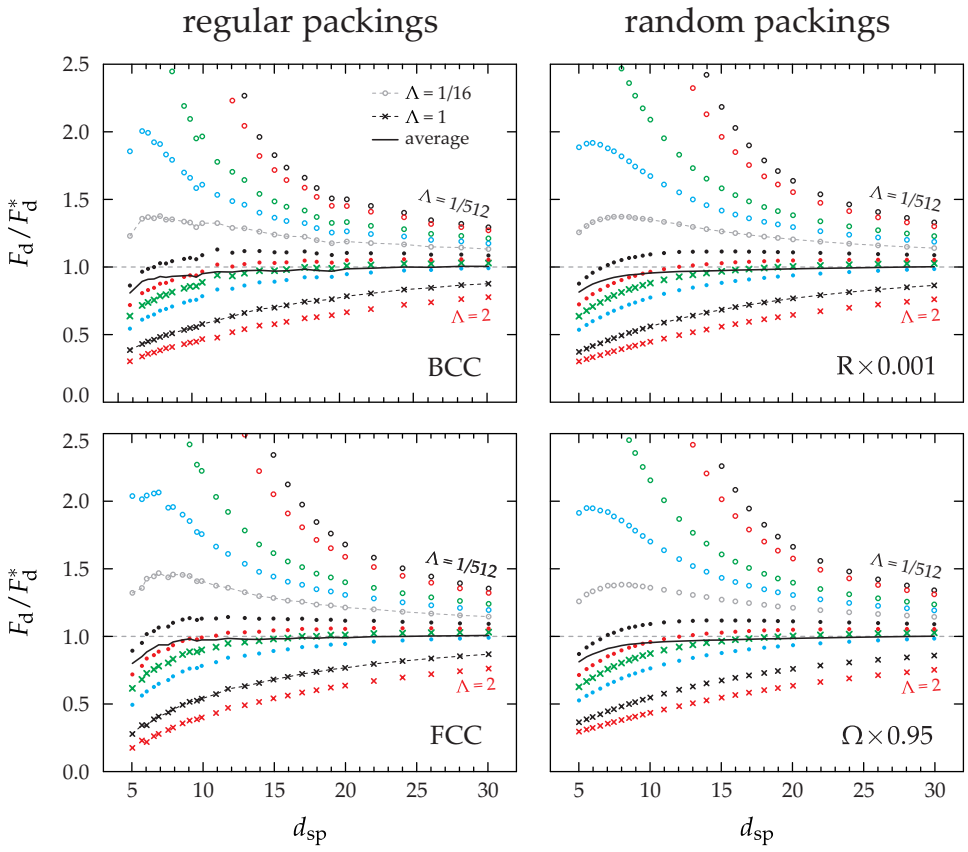

Figure 4. Dependence of the relative drag $F_d/F_d^\star$ on discretisation resolution for its lower considered values. The results are shown for $\Lambda = 1/512, 1/256, 1/64, 1/32, 1/16, 1/8, 3/16, 1/4, 3/8, 1, 2$. Some drag values obtained with $\Lambda \leq 1/64$ are not shown due to their larger magnitudes. Black solid line is the drag averaged from two relative drag values obtained with $\Lambda = 1/16$ and $\Lambda = 1$.

on F_d we split our analysis addressing separately high and low resolution regions. High resolution analysis revealed that F_d with virtually any Λ will first achieve some F_d value above the accurate solution and then, with further increase of the resolution, will continue converging to $F_d^\star$ at the rate of -1.0 or slower. Addressing lower resolution allowed us to suggest that instead of using any particular Λ value one can achieve higher accuracy after performing two simulations for a pair of (Λ_1, Λ_2) values and then averaging the result; our brief study suggests $\Lambda_1 = 1/16$ and $\Lambda_2 = 1$ to be a good candidate.

Our analysis in this paper is based on variation of spatial resolution within wide range. Although at a first glance higher resolutions are of purely academic interest, they are necessary to obtain complete picture of the solution behaviour (convergence) which later may open the possibility to predict higher resolution results by performing actual simulations in low-to-moderate resolution region only. Variation of the resolution is a very computationally demanding task because the computational effort grows as $O(d_{sp}^5)$ where $O(d_{sp}^3)$

comes from the increase of amount of mesh nodes to be processed on each iteration and $O(d_{\mathrm{sp}}^2)$ is due to the higher amount of iterations needed to achieve a given accuracy, which originates from the increase of the distance (in lattice units) between "solid" mesh nodes. In fact, the situation is even worse because at high resolutions the absolute error magnitude becomes small and the simulation accuracy must be further increased to accurately resolve systematic trends in the behaviour of errors with smaller magnitude. To be more specific about computational efforts, a single point in Fig. 3b for $d_{\mathrm{sp}} > 200$ required about 5 hours of calculation using 32768 processor cores.

References

1. S. Khirevich, I. Ginzburg, and U. Tallarek, *Coarse- and fine-grid numerical behavior of MRT/TRT lattice-Boltzmann schemes in regular and random sphere packings*, J. Comp. Phys. **281**, 708–742, 2015, DOI: 10.1016/j.jcp.2014.10.038.
2. W. S. Jodrey and E. M. Tory, *Computer simulation of isotropic, homogeneous, dense random packing of equal spheres*, Powder Technol. **30**, 111–118, 1981, DOI: 10.1016/0032-5910(81)80003-4.
3. S. Succi, *The lattice Boltzmann equation for fluid dynamics and beyond*, Oxford University Press, New York, 2001.
4. S. Chen and G. D. Doolen, *Lattice Boltzmann method with regularized non-equilibrium distribution functions*, Ann. Rev. Fluid Mech. **30**, 329–364, 1998, DOI: 10.1146/annurev.fluid.30.1.329.
5. D. d'Humiéres and I. Ginzburg, *Viscosity independent numerical errors for Lattice Boltzmann models: from recurrence equations to "magic" collision numbers*, Comp. Math. Appl. **58**, 823–840, 2009, DOI: 10.1016/j.camwa.2009.02.008.
6. I. Ginzbourg and P. M. Adler, *Boundaryow condition analysis for the three-dimensional lattice Boltzmann model*, J. Phys. II France **4**, 191–214, 1994, DOI: 10.1051/jp2:1994123.
7. D. d'Humiéres, I. Ginzburg, M. Krafczyk, P. Lallemand, and L.-S. Luo, *Multiple-relaxation-time lattice Boltzmann models in three dimensions*, Philos. Trans. R. Soc. A **360**, 437-451, 2002, DOI: 10.1098/rsta.2001.0955.
8. C. Pan, L.-S. Luo, and C. T. Miller, *An evaluation of lattice Boltzmann schemes for porous media simulation*, Comput. Fluids **35**, 898–909, 2006, DOI: 10.1016/j.compfluid.2005.03.008.
9. R. S. Maier, D. M. Kroll, Y. E. Kutsovsky, H. T. Davis, and R. S. Bernard, *Simulation of ow through bead packs using the lattice Boltzmann method*, Phys. Fluids **10**, 60–74, 1998, DOI: 10.1063/1.869550.
10. B. Bijeljic, P. Mostaghimi, and M. J. Blunt, *Insights into non-Fickian solute transport in carbonates*, Water Resour Res. **49**, 2714–2728, 2013, DOI: 10.1002/wrcr.20238.
11. L. Talon, D. Bauer, N. Gland, S. Youssef, H. Auradou, and I. Ginzburg, *Assessment of the two relaxation time Lattice-Boltzmann scheme to simulate Stokes flow in porous media*, Water Resour. Res. **48**, W04526, 2012, DOI: 10.1029/2011WR011385.